Biophysical Chemistry 136 (2008) 44–49

Contents lists available at ScienceDirect

Biophysical Chemistry

journal homepage: http://www.elsevier.com/locate/biophyschem

Anomalously high aggregation level of the polyene antibiotic amphotericin B in acidic medium: Implications for the biological action

Mariusz Gagoś [a,b], Monika Hereć [a,c], Marta Arczewska [b], Grzegorz Czernel [b], Mauro Dalla Serra [d], Wiesław I. Gruszecki [a,*]

[a] Department of Biophysics, Institute of Physics, Maria Curie-Skłodowska University, 20-031 Lublin, Poland
[b] Department of Physics, University of Live Science, 20-033 Lublin, Poland
[c] Department of Theoretical Physics, The John Paul II Catholic University of Lublin, Lublin, Poland
[d] FBK and CNR Institute of Biophysics, Unit at Trento, Via alla Cascata 56/C, 38100 Povo (Trento) Italy

ARTICLE INFO

Article history:
Received 17 February 2008
Received in revised form 15 April 2008
Accepted 15 April 2008
Available online 22 April 2008

Keywords:
Polyene antibiotics
Amphotericin B
Membrane channels
Molecular aggregates
Excitonic interactions

ABSTRACT

Amphotericin B (AmB) is a polyene antibiotic used to treat deep-seated mycoses. Both the therapeutic action and the toxic side effects of this drug are dependent on its molecular organization. AmB appears as a zwitterion at neutral pH owing to $-NH_3^+$ and $-COO^-$ groups. The results obtained with electronic absorption, fluorescence, resonance light scattering and infrared absorption spectroscopic analyses show that in the aqueous medium at pH above 10 AmB appears in the monomeric form owing to the negative net electric charge of the molecule. On the contrary, anomalously high aggregation level has been observed at pH below 2, despite the positive net electric charge. The effect is interpreted in terms of the permanent polarization of the polyene chain at low pH, associated with relative rotational freedom of the charged mycosamine fragment of the molecule. The pH-dependent aggregation of AmB is discussed in aspect of pharmacological action of the drug.

© 2008 Elsevier B.V. All rights reserved.

1. Introduction

Amphotericin B (AmB) is a lifesaving polyene antibiotic (see Fig. 1 for a chemical structure) used to treat deep-seated mycotic infections [1,2]. Owing to the amphiphilic molecular structure AmB is able to self-organize into molecular aggregates both in water phase and in the hydrophobic core of the lipid membranes [3–7]. In the latter case, AmB is postulated to self-aggregate into the hydrophilic pores that may severely affect transmembrane ion transport [8–10]. On the other hand, the results of the recent structural studies show that the pharmacological effect of AmB towards the membranes may be associated with modification of structural and dynamic properties of the lipid bilayer [11–14]. Despite the exact mode of action of AmB it is without doubt that both the pharmacological activity and the toxic side effects are strongly dependent on molecular organization of the drug in formulation [1,15–17]. Several delivery systems and modifications of the antibiotic molecule have been elaborated to reduce the toxic side effects. Among others, the cationic derivatives of AmB have been proposed to be good candidates for an antibiotic with reduced toxicity to patients [7,18–22]. The cationic form of AmB can be obtained in aqueous solution by decreasing pH below the pK_a value of the amino group, close to 3 [7]. In the present report we show that under such conditions AmB forms strongly-coupled aggregated structures composed out of the antiparallel dimers. Low toxicity of such a system may be based upon the fact that antiparallel dimers are not able to assemble directly into the molecular porous structures.

2. Materials and methods

Amphotericin B (AmB) in a crystalline form was purchased from Sigma Chem. Co. AmB was dissolved in deionized (mQ) water, alkalized to pH 12 with KOH and then centrifuged for 15 min at 15,000×g in order to remove micro-crystals of the drug still remaining in the sample. The final concentration of AmB was calculated from the absorption spectra on the basis of the molar extinction coefficient 1.05×10^5 M^{-1} cm^{-1} (0–0 absorption maximum at 408 nm). Light absorption measurements were carried out with a double-beam UV–Vis spectrophotometer Cary 300 Bio from Varian equipped with thermostatted cuvette holder with 6×6 multicell block Peltier. Absorption spectra were recorded at 25±1 °C. The temperature was controlled with thermocouple probe (Cary Series II from Varian) placed directly within the sample. Fluorescence excitation, emission and synchronous spectra were recorded with a Schimadzu RF-5001-PC spectrofluorometer and with a SPEX Fluoromax spectrofluorometer from HORIBA Jobin Ivon. Fluorescence spectra were recorded with 0.5 nm resolution and corrected for the lamp and photomultiplier spectral characteristics. The excitation and emission slits were set to 2 and

* Corresponding author. Tel.: +48 81 537 62 52; fax: +48 81 537 61 91.
E-mail address: wieslaw.gruszecki@umcs.lublin.pl (W.I. Gruszecki).

0301-4622/$ – see front matter © 2008 Elsevier B.V. All rights reserved.
doi:10.1016/j.bpc.2008.04.005

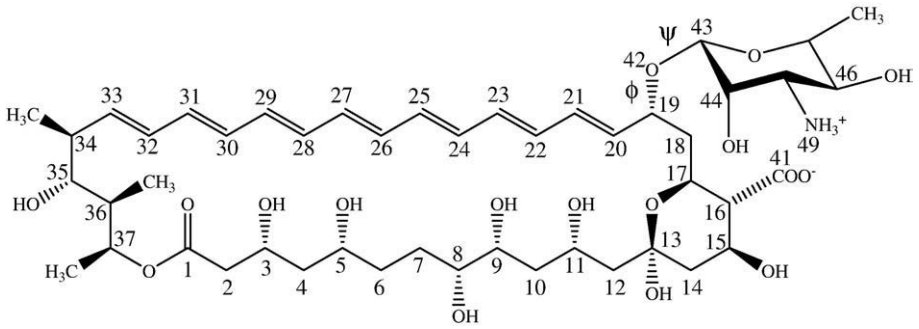

Fig. 1. Chemical structure of amphotericin B (AmB).

5 nm in the case of recording fluorescence excitation spectra and to 5 and 2 nm in the case of recording fluorescence emission spectra, respectively. Resonance light scattering measurements were performed as in Pasternack and Collings [23]. The excitation and emission monochromators of the spectrofluorimeter were scanned synchronously (0.0 nm interval between excitation and emission wavelength), the slits were set to 1 nm.

Infrared absorption spectra were recorded with the Fourier-transform infrared (FTIR) spectrometer, model Bio-Rad FTS 185, equipped with a MCT detector and KBr beamsplitter. Before the measurements the instrument was purged with CO_2-free dry air for 30 min. The attenuated total reflection (ATR) configuration was used with a 10-reflections Ge crystal (45° cut). The Teflon dish was also used, where the crystal was deposited with both sides' hermetic reservoirs for water solution. Typically 100 interferograms were collected, Fourier transformed and averaged. Absorption spectra in the region between 4000 and 600 cm^{-1}, at a resolution of one data point every 1 cm^{-1}, were obtained using a clean crystal as the background. ATR crystals were cleaned with organic solvents and for 30 min by "Harrick" Plasma Cleaner. Spectral analysis was performed with Grams/AI software from ThermoGalactic (USA).

3. Results and discussion

Fig. 2 presents electronic absorption spectra of AmB dissolved in aqueous medium at pH 5.0 and the same solution acidified to pH 2.0 and alkalized to pH 12.0. As can be seen, the absorption spectrum of AmB solution prepared originally in the aqueous medium at pH 5.0 displays a broad absorption band in the short-wavelength region, superimposed on the electronic absorption band with characteristic vibrational sub-structure, typical for polyenes. The short-wavelength spectral band, observed is diagnostic of molecular aggregates [4,6,21,24] indicates that at pH 5.0 the drug appears, at least partially, in the aggregated form. Interestingly, the alkalization of the medium results in complete monomerization of AmB in the sample. Such an effect can be readily explained in terms of electrostatic repulsion of the negatively charged molecules [21]. AmB is a zwitterion in neutral pH. The zwitterionic state of AmB results from the positively charged amino group ($-NH_3^+$) and negatively charged carboxyl group ($-COO^-$). The pK_a of the amino group of AmB has been found to be close to 9 and therefore the molecules are expected to appear largely as anions, at high pH values [21]. Fig. 3 presents the pH dependence of a ratio of absorbance of aqueous AmB sample, recorded at 336 nm (at the center of the aggregation-related band) and at 408 nm (maximum of the monomeric form). As can be expected, the aggregation level of AmB decreases at pH values in which the antibiotic molecule possesses net electric charge: at pH higher than 10 (above the pK_a value for the amino group) and at pH lower than 3 (below the pK_a value of the carboxyl group [21]). Surprisingly, the aggregation level of AmB in the samples acidified to pH values below 2 started to rise again in course of further acidification. Moreover, the aggregation level exceeded considerably the aggregation level of the drug observed at neutral pH values, despite the positive net electric charge on the molecule. Very similar behavior can be observed while analyzing the level of dimerization of AmB in the same samples. Monitoring of the level of AmB dimer is possible owing to the distinct spectral signature of the dimeric structures in the fluorescence excitation and emission spectra, different from the

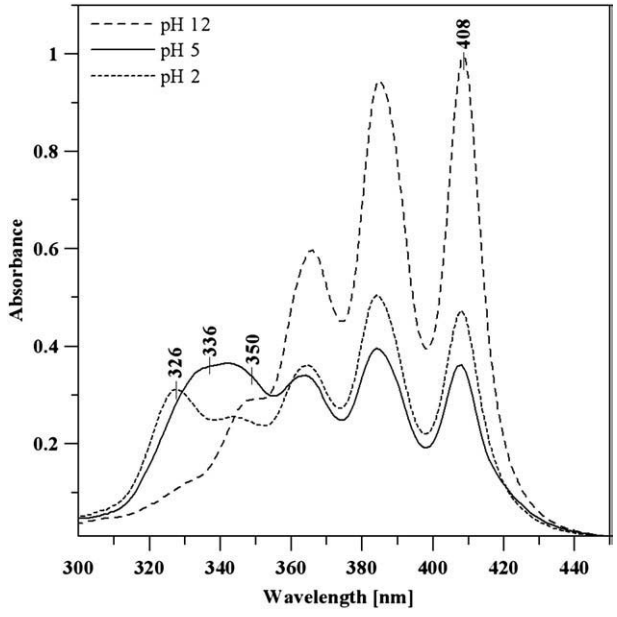

Fig. 2. Absorption spectra of AmB in aqueous medium at different pH values, indicated.

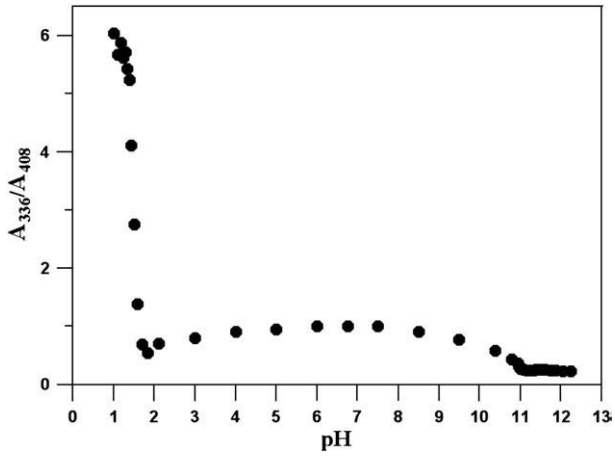

Fig. 3. The pH dependence of the absorbance ratio at 336 (aggregated form) and 408 nm (monomeric form) in the absorption spectrum of AmB. The ratio (A_{336}/A_{408}) corresponds to the level of aggregation.

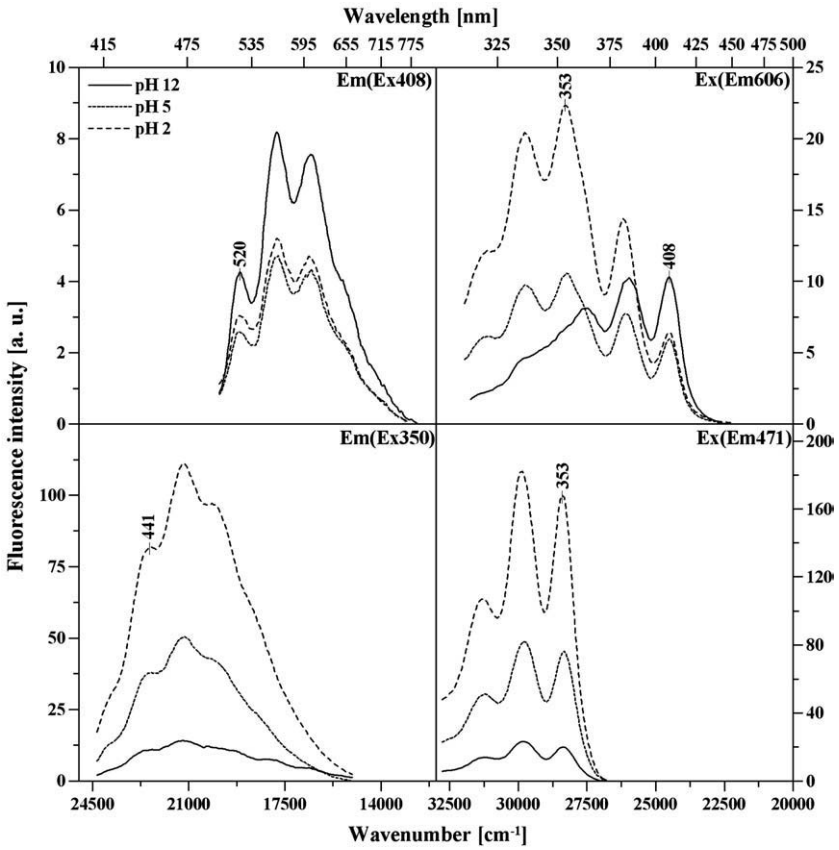

Fig. 4. Fluorescence excitation (Ex) and emission (Em) spectra of AmB dissolved in the aqueous medium at different pH conditions. The main spectral bands are the following: in the excitation spectrum (Em 606 nm) at 320, 333, 353, 385 and 408 nm; in the emission spectrum (Ex 408 nm) at 520, 563, and 606 nm; in the excitation spectrum (Em 471 nm) at 320, 334, 353 nm; in the emission spectrum (Ex 350 nm) at 441, 473 and 502 nm.

spectra of monomeric and aggregated AmB [25–27] (Fig. 4). Fig. 5 presents the pH dependency of AmB dimer to monomer ratio. As can be seen, the anomalously high molecular association level of AmB at pH values below 2, has been also observed in the case of dimer formation. In order to understand this apparent paradox, AmB samples were subjected to vibrational spectroscopic analysis with application of the FTIR technique. Fig. 6 presents the infrared absorption spectra of AmB in aqueous samples at different pH. The three different spectral regions were analyzed, relevant for molecular organization of AmB. Relatively strong, broad absorption band centered at 3310 cm^{-1}, visible in the spectrum recorded at pH 12 (panel A) and assigned to the C–N stretching vibrations in the NH_2 group is replaced by the band shifted towards lower wavenumbers by ca. 370 cm^{-1}, recorded at lower pH, assigned to the C–N stretching vibrations in the NH_3^+ group. This spectral feature is diagnostic of the pH-induced protonation of the NH_2 group [28]. Interestingly, this spectral band appears exceptionally narrow at pH values below 2 (see Fig. 6D). The pair of bands centered at 1671 cm^{-1} and 1393 cm^{-1} represents respectively the antisymmetric and symmetric C–O stretching vibrations in the $-COO^-$ group. On the other hand, the band pair at ca. 1710 cm^{-1} and 1620 cm^{-1} can be assigned, respectively, to the antisymmetric and symmetric stretching vibrations of the hydrogen-bonded –C=O group in the non-ionized carboxyl. The appearance of these spectral bands and simultaneous disappearance of the bands assigned to the ionized carboxyl group, in response to the pH decrease, is directly associated with and reflects the protonation of the $-COO^-$ group of AmB [28]. Interestingly, the relatively low intensity band visible at 1561 cm^{-1} at pH 12, which can be assigned to the C=C stretching vibrations in the polyene chain of AmB, becomes shifted towards lower energies along with the pH decrease. Such a spectral effect can be interpreted in terms of the polyene–polyene interactions leading to aggregation of AmB molecules. At the same time, the bands attributed to the skeletal vibrations of the molecule: δ C–H (1071 cm^{-1}) and δ C–C–H (1012 cm^{-1}) distinctly gain their intensity. One of the possible explanations of this spectral effect can be based upon molecular aggregation-induced deformation of the AmB molecules that results in the increase of the electron dipole transition of these particular skeletal vibrations. It can be expected that in the broad pH range, the relative rotational freedom

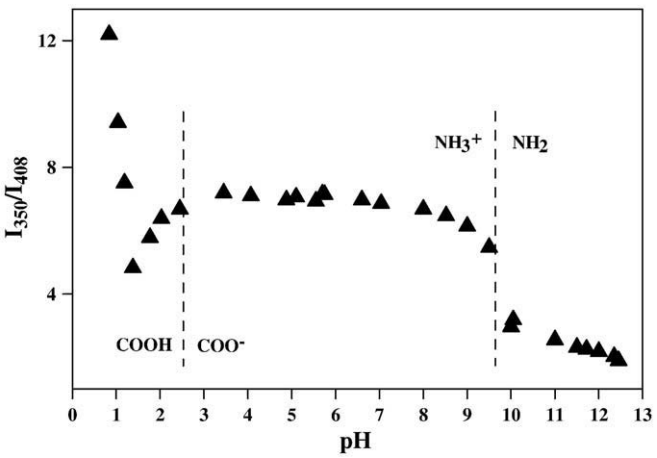

Fig. 5. Fluorescence intensity ratio (Ex at 350 nm, Em at 471 nm and Ex at 408 nm, Em at 606 nm) corresponding to the ratio of emission due to the dimeric to that of monomeric form of AmB as a function of pH.

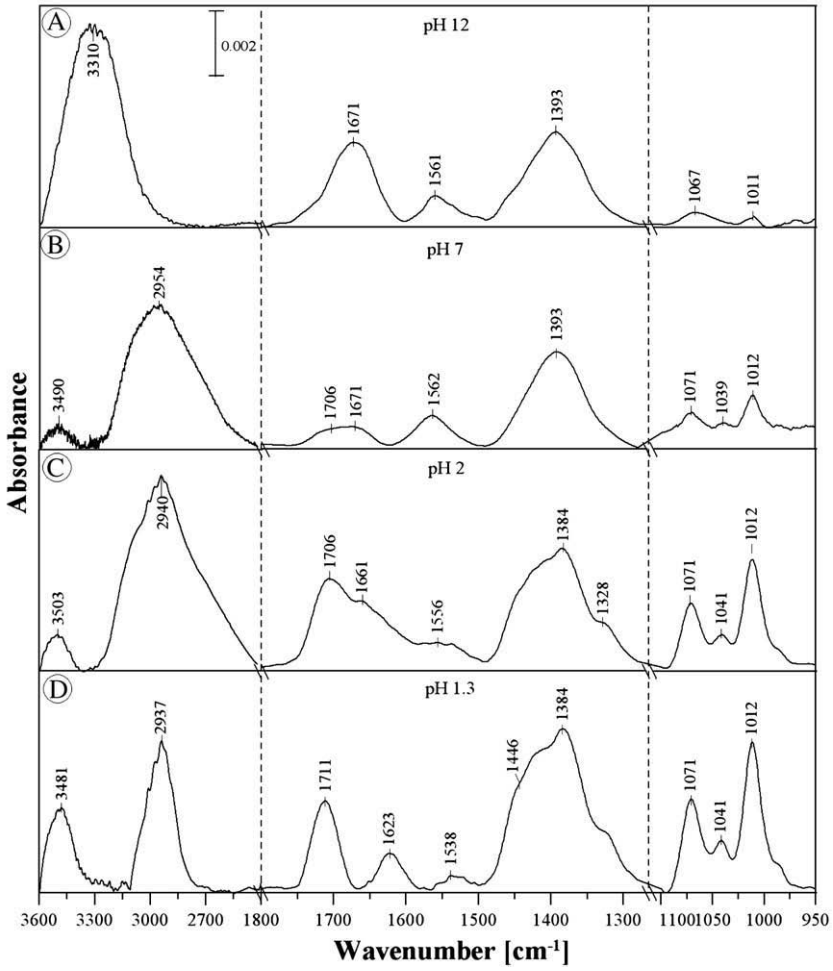

Fig. 6. ATR-FTIR absorption spectra recorded from AmB dissolved in water solution at different pH values, indicated. Sample was deposited at the two sides of a Ge crystal placed in the hermetic Teflon dish. Concentration of AmB in the sample 10^{-5}M.

of the mycosamine moiety around the C19–O42 and O42–C43 bonds (the torsion angles Φ and Ψ respectively [29], see Fig. 1) is restricted owing to the steric hindrance [29] but also owing to the electrostatic coupling or intramolecular hydrogen bond formation between the $-NH_3^+$ and $-COO^-$ groups. Such freedom can be restored at higher and lower pH, when one of the groups loses its electric charge. In the case of low pH values possible rotation of the positively charged mycosamine shell considerably affects electric charge distribution along the conjugated double bond system of the polyene chain of AmB molecule. Creation of a permanent dipole moment of the polyene (higher electron density on the side of positively charged mycosamine) would result in higher affinity of the molecules to bind one to each other via the chromophore–chromophore interactions. Formation of antiparallel AmB dimers, called also head-to-tail dimers [30–32], would be highly probable due to the antiparallel orientation of the attracting electric dipoles. According to the general conviction, the aggregated structures of AmB are composed of dimers [7]. It seems unlikely that such antiparallel dimers would assemble into porous structures. On the other hand, one can expect that the chromophore–chromophore distance in such a dimeric structure shall be relatively short and therefore the excitonic interactions in the aggregated structures built out of such dimers shell result in a pronounced hypsochromic shift of the absorption spectrum [25]. Indeed, as can be seen the short-wavelength absorption maximum attributed to the aggregated structure appears at 326 nm in the AmB aqueous sample at pH 2.0, in contrast to the other aggregated forms of AmB, characterized by the short-wavelength maxima in the region between 330 and 350 nm. The aggregated structure of AmB that gives rise to such a strong hypsochromic shift has been observed in the samples of the drug subjected to heating at temperatures above 50 °C and such a structure has been named "superaggregate" [5]. Better characterization of the localization of aggregation-related excitonic energy

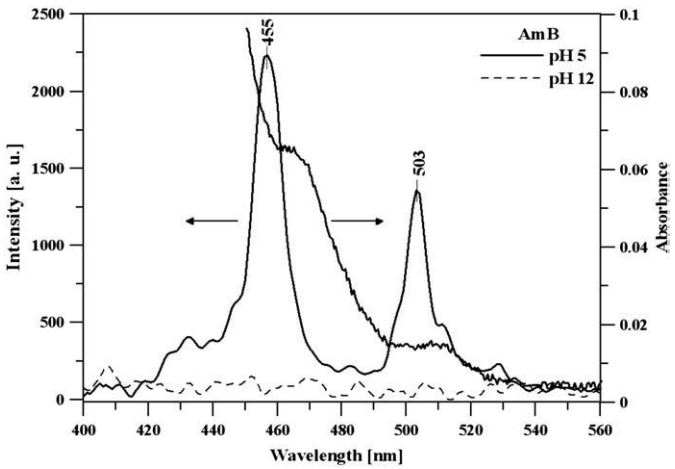

Fig. 7. RLS spectra of the aqueous solution of AmB at pH 5.0 (solid line) and alkalized to pH 12 (dotted line). Two spectral bands peaking at 455 nm and 503 nm are present only in the sample containing aggregated AmB. Relatively low intensity spectral features (right scale) in the absorption spectra of the same sample can be observed, corresponding to the bands in the RLS spectra.

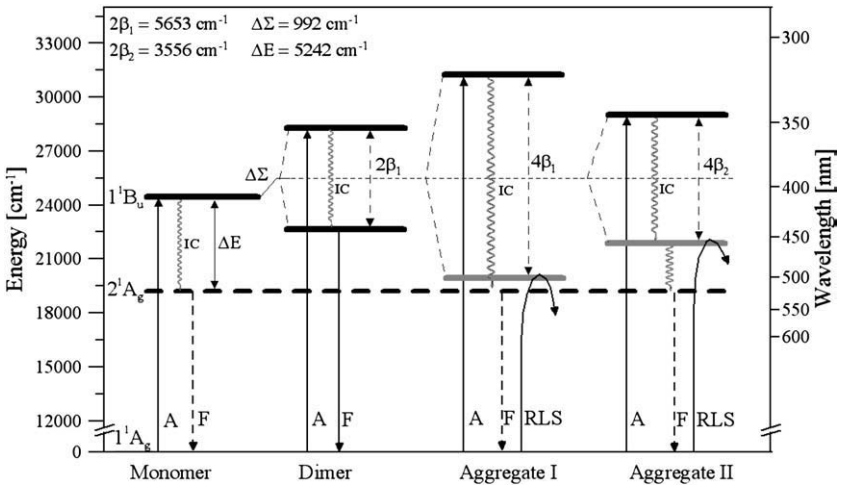

Fig. 8. Diagram of the energy levels of AmB in monomeric, dimeric and aggregated (Aggregate I and Aggregate II) forms, based on the spectroscopic analysis (Figs. 2, 4, and 7). The low energy levels of aggregated AmB, observed at 455 nm and 503 nm (gray line), correspond to the high energy levels that are responsible for light absorption at 336 nm and 326 nm. A denotes absorption, F fluorescence, IC internal conversion, RLS resonance light scattering.

levels is possible with application of the resonance light scattering (RLS) technique owing to the fact that low-lying excitonic energy levels give rise to the RLS signal, even when contribution of such energy levels to electronic absorption spectra is sometimes very low [23,33,34]. Fig. 7 presents the RLS spectra of the aqueous solution of AmB at pH 5.0 and alkalized to pH 12. Two pronounced RLS spectral bands can be seen, peaking at 455 nm and 503 nm, exclusively in the sample containing aggregated AmB. Relatively low intensity spectral features in the absorption spectra of the same sample can be observed, corresponding to the bands in the RLS spectra. The existence of two separate RLS bands in the low energy spectral region indicates that two different aggregated structures of AmB are present in the sample, characterized by different dipole–dipole coupling energies β. Fig. 8 presents the diagram of the energy levels of AmB in monomeric and dimeric forms, based on the absorption and fluorescence spectra and also excitation energy levels of AmB in two types of aggregated structures formed. As it directly follows from the diagram, the low energy levels of aggregated AmB, observed at 455 nm and 503 nm, correspond to the high energy levels, that are responsible for light absorption at 336 nm and 326 nm respectively, observed in the short-wavelength region of the absorption spectra (Fig. 2). It is therefore highly probable that the Aggregate I, characterized by the strong coupling, is composed out of antiparallel dimers of AmB, preferentially formed at low pH. The second aggregated structure (the Aggregate II, Fig. 8), characterized by the lower interaction energy (most probably owing to higher distance between the chromophores) may represent the structure composed of parallel-arranged dimers, able to form molecular pores. Interestingly, the spectral shifts observed in the case of the Aggregate I are exactly double (in energy units) of the spectral shift observed in the case of the dimeric structures ($4\beta_1$ versus $2\beta_1$, see Fig. 8). This means that the dimers of AmB are composed of head-to-tail-oriented molecules and that such dimers are constituents of the strongly-coupled molecular forms of the Aggregate I.

The results of the present research show that acidity of the medium can drastically influence molecular organization of AmB. Three essentially different organization forms of the drug can be achieved in an aqueous medium: monomers, at pH above 10, strongly-coupled aggregated structures at pH below 2 and weakly-coupled aggregated structures in the pH range 3–10. From the pharmacological point of view, the weakly-coupled aggregates of AmB seem to be associated with high risk of toxic side effects, owing to the fact that such structures may directly assemble into the porous structures that are able to affect the physiological transmembrane ion transport. The dependency of AmB organization of medium acidity may be advantageous in elaboration of delivery formulas of the drug, characterized by reduced toxicity for patients.

Acknowledgements

This research was financed by the Ministry of Education and Science of Poland from the budget funds for science in the years 2004–2007 within the research project 2P05F04327. MG acknowledges Instituto Trentino di Cultura for granting a short term research fellowship.

References

[1] J.J. Torrado, R. Espada, M.P. Ballesteros, S. Torrado-Santiago, Amphotericin B formulations and drug targeting, J. Pharm. Sci (in press). Published online in Wiley InterScience (www.interscience.wiley.com). doi:10.1002/jps.21179.
[2] M. Baginski, B. Cybulska, W.I. Gruszecki, Interaction of macrolide antibiotics with lipid membranes, in: A. Ottova-Liu (Ed.), Advances in Planar Lipid Bilayers and Liposomes, 3, Elsevier Science Publ., Amsterdam, 2006, pp. 269–329.
[3] M. Baginski, H. Resat, J.A. McCammon, Molecular properties of amphotericin B membrane channel: a molecular dynamics simulation, Mol. Pharmacol. 52 (1997) 560–570.
[4] J. Barwicz, W.I. Gruszecki, I. Gruda, Spontaneous organization of amphotericin B in aqueous medium, J. Colloid. Interf. Sci. 158 (1993) 71–76.
[5] F. Gaboriau, M. Cheron, L. Leroy, J. Bolard, Physico-chemical properties of the heat-induced 'superaggregates' of amphotericin B, Biophys. Chem. 66 (1997) 1–12.
[6] W.I. Gruszecki, M. Gagos, M. Herec, P. Kernen, Organization of antibiotic amphotericin B in model lipid membranes. A mini review, Cell. Mol. Biol. Lett. 8 (2003) 161–170.
[7] J. Mazerski, J. Grzybowska, E. Borowski, Influence of net charge on the aggregation and solubility behaviour of amphotericin B and its derivatives in aqueous media, Eur. Biophys. J. 18 (1990) 159–164.
[8] B. De Kruijff, W.J. Gerritsen, A. Oerlemans, R.A. Demel, L.L. van Deenen, Polyene antibiotic-sterol interactions in membranes of *Acholeplasma laidlawii* cells and lecithin liposomes. I. Specificity of the membrane permeability changes induced by the polyene antibiotics, Biochim. Biophys. Acta 339 (1974) 30–43.
[9] W.I. Gruszecki, M. Gagos, P. Kernen, Polyene antibiotic amphotericin B in monomolecular layers: spectrophotometric and scanning force microscopic analysis, FEBS. Lett. 524 (2002) 92–96.
[10] M. Herec, H. Dziubinska, K. Trebacz, J.W. Morzycki, W.I. Gruszecki, An effect of antibiotic amphotericin B on ion transport across model lipid membranes and tonoplast membranes, Biochem. Pharmacol. 70 (2005) 668–675.
[11] I. Fournier, J. Barwicz, M. Auger, P. Tancrede, The chain conformational order of ergosterol- or cholesterol-containing DPPC bilayers as modulated by Amphotericin B: a FTIR study, Chem. Phys. Lipids. 151 (2008) 41–50.
[12] J. Gabrielska, M. Gagos, J. Gubernator, W.I. Gruszecki, Binding of antibiotic amphotericin B to lipid membranes: a 1H NMR study, FEBS. Lett. 580 (2006) 2677–2685.
[13] M. Gagos, J. Gabrielska, M. Dalla Serra, W.I. Gruszecki, Binding of antibiotic amphotericin B to lipid membranes: monomolecular layer technique and linear dichroism-FTIR studies, Molec. Memb. Biol. 22 (2005) 433–442.
[14] M. Herec, A. Islamov, A. Kuklin, M. Gagos, W.I. Gruszecki, Effect of antibiotic amphotericin B on structural and dynamic properties of lipid membranes formed with egg yolk phosphatidylcholine, Chem. Phys. Lipids. 147 (2007) 78–86.

[15] J. Barwicz, S. Christian, I. Gruda, Effects of the aggregation state of amphotericin B on its toxicity to mice, Antimicrob. Agents. Chemother. 36 (1992) 2310–2315.
[16] J. Barwicz, I. Dumont, C. Ouellet, I. Gruda, Amphotericin B toxicity as related to the formation of oxidatively modified low-density lipoproteins, Biospectroscopy 4 (1998) 135–144.
[17] J. Brajtburg, W.G. Powderly, G.S. Kobayashi, G. Medoff, Amphotericin B: delivery systems, AntimicrobAgents Chemother. (1990) 381–384.
[18] I. Blanc, M. Saint-Pierre Chazalet, Oligonucleotide delivery by a cationic derivative of the polyene antibiotic amphotericin B. II: study of the interactions of the oligonucleotide/cationic vector complexes with lipid monolayers and lipid unilamellar vesicles, Biochim. Biophys. Acta. 1464 (2000) 309–321.
[19] K. Hac-Wydro, P. Dynarowicz-Latka, J. Grzybowska, E. Borowski, Interactions of amphotericin B derivative of low toxicity with biological membrane components—the Langmuir monolayer approach, Biophys. Chem. 116 (2005) 77–88.
[20] K. Kasumov, J. Bolard, Transient permeability induced by cationic derivatives of amphotericin B in lipid membranes, Pol. J. Chem. 78 (2004) 1057–1065.
[21] J. Mazerski, J. Bolard, E. Borowski, Effect of the modifications of ionizable groups of amphotericin B on its ability to form complexes with sterols in hydroalcoholic media, Biochim. Biophys. Acta. 1236 (1995) 170–176.
[22] M. Toledo Grijalba, M. Cheron, E. Borowski, J. Bolard, S. Schreier, Modulation of polyene antibiotics self-association by ions from the Hofmeister series, Biochim. Biophys. Acta. 1760 (2006) 973–979.
[23] R.F. Pasternack, P.J. Collings, Resonance light scattering: a new technique for studying chromophore aggregation, Science 269 (1995) 935–939.
[24] P. Tancrede, J. Barwicz, S. Jutras, I. Gruda, The effect of surfactants on the aggregation state of amphotericin B, Biochim. Biophys. Acta. 1030 (1990) 289–295.
[25] W.I. Gruszecki, M. Gagos, M. Herec, Dimers of polyene antibiotic amphotericin B detected by means of fluorescence spectroscopy: molecular organization in solution and in lipid membranes, J. Photochem. Photobiol. B:. Biol. 69 (2003) 49–57.
[26] W.I. Gruszecki, M. Herec, Dimers of polyene antibiotic amphotericin B, J. Photochem. Photobiol. B:. Biol. 72 (2003) 103–105.
[27] R. Stoodley, K.M. Wasan, D. Bizzotto, Fluorescence of amphotericin B-deoxycholate (fungizone) monomers and aggregates and the effect of heat-treatment, Langmuir 23 (2007) 8718–8725.
[28] S. Olsztyńska, M. Komorowska, L. Vrielynck, N. Dupuy, Vibrational spectroscopic study of L-phenylalanine: effect of pH. Appl. Spectrosc. 55 (2001) 901–907.
[29] J. Czub, E. Borowski, M. Baginski, Interactions of amphotericin B derivatives with lipid membranes—a molecular dynamics study, Biochim. Biophys. Acta. 1768 (2007) 2616–2626.
[30] M. Baginski, E. Borowski, Distribution of electrostatic potential around amphotericin B and its membrane targets, Theochem-J. Mol. Struct. 389 (1997) 139–146.
[31] J. Caillet, J. Berges, J. Langlet, Theoretical study of the self-association of amphotericin B, Biochim. Biophys. Acta 1240 (1995) 179–195.
[32] J. Mazerski, E. Borowski, Molecular dynamics of amphotericin B. II. Dimer in water, Biophys. Chem. 57 (1996) 205–217.
[33] J.C. de Paula, J.H. Robblee, R.F. Pasternack, Aggregation of chlorophyll a probed by resonance light scattering spectroscopy, Biophys. J. 68 (1995) 335–341.
[34] J. Parkash, J.H. Robblee, J. Agnew, E. Gibbs, P. Collings, R.F. Pasternack, J.C. de Paula, Depolarized resonance light scattering by porphyrin and chlorophyll a aggregates, Biophys. J. 74 (1998) 2089–2099.